Available online at www.sciencedirect.com
SCIENCE DIRECT®
Physics Letters A 334 (2005) 160–168
PHYSICS LETTERS A
www.elsevier.com/locate/pla

# Mechanism for boundary crises in quasiperiodically forced period-doubling systems

Sang-Yoon Kim, Woochang Lim *

*Department of Physics, Kangwon National University, Chunchon, Kangwon-Do 200-701, South Korea*

Received 14 June 2004; accepted 3 November 2004

Available online 24 November 2004

Communicated by A.R. Bishop

**Abstract**

We investigate the mechanism for boundary crises in the quasiperiodically forced logistic map which is a representative model for quasiperiodically forced period-doubling systems. For small quasiperiodic forcing $\varepsilon$, a chaotic attractor disappears suddenly via a "standard" boundary crisis when it collides with the smooth unstable torus. However, when passing a threshold value of $\varepsilon$, a basin boundary metamorphosis occurs, and then the smooth unstable torus is no longer accessible from the interior of the basin of the attractor. For this case, using the rational approximations to the quasiperiodic forcing, it is shown that a nonchaotic attractor (smooth torus or strange nonchaotic attractor) as well as a chaotic attractor is destroyed abruptly through a new type of boundary crisis when it collides with an invariant "ring-shaped" unstable set which has no counterpart in the unforced case.



*PACS:* 05.45.Ac; 05.45.Df; 05.45.Pq

*Keywords:* Quasiperiodically forced systems; Boundary crisis

## 1. Introduction

Dynamical transitions of attractors occurring as the system parameters are changed have received much attention. In particular, sudden qualitative changes in the attractor are of special interest. Such discontinuous abrupt changes, called the crises, were first extensively studied by Grebogi et al. [1] and two kinds of crises were discovered for the case of chaotic attractors. A sudden disappearance of a chaotic attractor occurs when it collides with an unstable periodic orbit on its basin boundary, and is called the boundary crisis. On the other hand, an abrupt increase in the size of a chaotic attractor takes place when the unstable periodic orbit with which the chaotic attractor collides lies in the interior of the basin, and is called the interior crisis. Transient or intermittent dynamics associated with the boundary or interior crisis has been well charac-

* Corresponding author.
*E-mail addresses:* sykim@kangwon.ac.kr (S.-Y. Kim), wclim@kwnu.kangwon.ac.kr (W. Lim).

0375-9601/$ – see front matter 
doi:10.1016/j.physleta.2004.11.004

terized [2], and these crises have often been observed experimentally in periodically forced systems [3].

In this Letter, we study the boundary crisis (BC) in quasiperiodically forced systems driven at two incommensurate frequencies. These dynamical systems have attracted much attention because of typical appearance of strange nonchaotic attractors (SNAs) which are strange (fractal) but nonchaotic (no positive Lyapunov exponent) [4]. Since the first description of SNAs by Grebogi et al. [5], dynamical behaviors of the quasiperiodically forced systems have been extensively investigated both theoretically [6–22] and experimentally [23]. In a recent work [20], Osinga and Feudel investigated the BC in the quasiperiodically forced Hénon map, and observed a new type of BC that occurs when the smooth unstable torus is inaccessible from the interior of the basin of the attractor due to the basin boundary metamorphosis [24]. However, the unstable orbit inducing such a BC was not located, and thus the mechanism for the new BC remains unclear.

This Letter is organized as follows. In Section 2, we investigate the underlying mechanism for the BC in the quasiperiodically forced logistic map which we regard as a representative model for quasiperiodically forced period-doubling systems. For small quasiperiodic forcing $\varepsilon$, a sudden destruction of a chaotic attractor occurs through a "standard" BC when it collides with the smooth unstable torus which is developed from the unstable periodic orbit in the (unforced) logistic map. However, as $\varepsilon$ passes a threshold value, a basin boundary metamorphosis occurs, and then the smooth unstable torus loses its accessibility from the interior of the basin of the attractor. For this case, the type of the BC changes. Using the rational approximations (RAs) to the quasiperiodic forcing, it is shown that a nonchaotic attractor (smooth torus or SNA) as well as a chaotic attractor disappears suddenly via a new type of BC when it collides with an invariant "ring-shaped" unstable set on the basin boundary. Such a ring-shaped unstable set has no counterpart in the unforced case [22]. Finally, a summary is given in Section 3.

## 2. Boundary crises in the quasiperiodically forced logistic map

We study the mechanism for the BC in the quasiperiodically forced logistic map $M$, often used as a representative model for the quasiperiodically forced period-doubling systems:

$$M: \begin{cases} x_{n+1} = a - x_n^2 + \varepsilon \cos 2\pi\theta_n, \\ \theta_{n+1} = \theta_n + \omega \pmod 1, \end{cases} \tag{1}$$

where $x \in [0, 1]$, $\theta \in S^1$, $a$ is the nonlinearity parameter of the logistic map, and $\omega$ and $\varepsilon$ represent the frequency and amplitude of the quasiperiodic forcing, respectively. This quasiperiodically forced logistic map $M$ is noninvertible, because its Jacobian determinant becomes zero along the critical curve, $L_0 = \{x = 0, \theta \in [0, 1)\}$. Critical curves of rank $k$, $L_k$ $(k = 1, 2, \ldots)$, are then given by the images of $L_0$ (i.e., $L_k = M^k(L_0)$). Segments of these critical curves can be used to define a bounded trapping region of the phase space, called an "absorbing area", inside which, upon entering, trajectories are henceforth confined [25].

Here, we set the frequency to be the reciprocal of the golden mean, $\omega = (\sqrt{5} - 1)/2$, and then investigate the BC using the RAs. For the inverse golden mean, its rational approximants are given by the ratios of the Fibonacci numbers, $\omega_k = F_{k-1}/F_k$, where the sequence of $\{F_k\}$ satisfies $F_{k+1} = F_k + F_{k-1}$ with $F_0 = 0$ and $F_1 = 1$. Instead of the quasiperiodically forced system, we study an infinite sequence of periodically forced systems with rational driving frequencies $\omega_k$. We suppose that the properties of the original system $M$ may be obtained by taking the quasiperiodic limit $k \to \infty$.

Fig. 1 shows a phase diagram in the $a$–$\varepsilon$ plane. Each phase is characterized by both the Lyapunov exponent $\sigma_x$ in the $x$-direction and the phase sensitivity exponent $\delta$. The exponent $\delta$ measures the sensitivity with respect to the phase of the quasiperiodic forcing and characterizes the strangeness of an attractor in a quasiperiodically driven system [9]. A smooth torus has a negative Lyapunov exponent and no phase sensitivity ($\delta = 0$). Its region is denoted by $T$ and shown in light gray. When crossing the solid line, the smooth torus becomes unstable and bifurcates to a smooth doubled torus in the region denoted by $2T$. On the other hand, chaotic attractors have positive Lyapunov exponents and its region is shown in black. Between these regular and chaotic regions, SNAs that have negative Lyapunov exponents and high phase sensitivity ($\delta > 0$) exist in the region shown in gray. Due to their high phase sensitivity, these SNAs have fractal

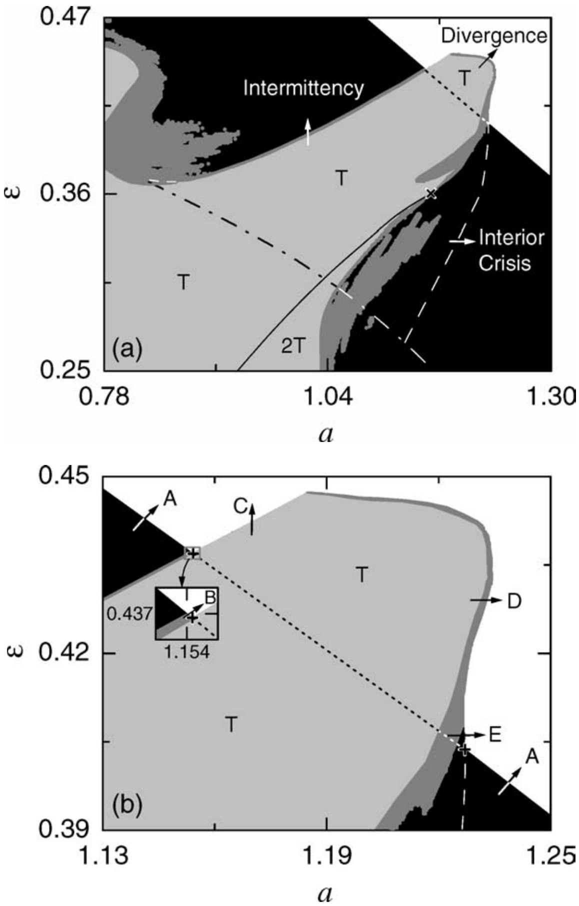


Fig. 1. (a) Phase diagram in the $a$–$\varepsilon$ plane. Regular, chaotic, SNA, and divergence regimes are shown in light gray, black, gray, and white, respectively. For the case of regular attractor, a torus and a doubled torus exist in the regions denoted by $T$ and $2T$, respectively. We note the existence of a "tongue" of quasiperiodic motion near the terminal point (marked with the cross) of the torus doubling bifurcation curve represented by the solid line. In this tongue, typical dynamical transitions such as the intermittency, interior crisis (occurring when passing the dashed line) and BC may occur through interaction with the ring-shaped unstable set born when passing the dash-dotted line. When passing the dotted line, a basin boundary metamorphosis occurs, and then the smooth unstable torus becomes inaccessible from the basin of the attractor. (b) BCs leading to divergence. A sudden destruction of a chaotic attractor (SNA) occurs via a "standard" BC along the route A (B) when it collides with the smooth unstable torus. On the other hand, through collision with a ring-shaped unstable set, a new type of BCs, which cause the abrupt destruction of the smooth torus, SNA, and chaotic attractors, occur along the routes C, D, and E, respectively. Hence, the BC curve is not differentiable at the two double-crisis vertices, denoted by the plus. A small box near the upper double-crisis vertex is magnified. For other details, see the text.

structure. This phase diagram is typical for quasiperiodically forced period-doubling systems [16–20,22]. Note that its main interesting feature is the existence of the "tongue" of quasiperiodic motion that penetrates into the chaotic region and separates it into upper and lower parts. We also note that this tongue lies near the terminal point (denoted by the cross) of the torus doubling bifurcation curve. In this tongue, rich dynamical transitions such as intermittency, interior crisis, and BC occur. Here, we are interested in the BC inducing divergence that occurs in the region shown in white.

We first consider a BC occurring along the route $A$ ($\varepsilon = 0.5a - 0.28$) in Fig. 1(b). A chaotic attractor, bounded by the critical curves $L_k$ ($k = 1, \dots, 4$), is given in Fig. 2(a) for $a = 1.19$ and $\varepsilon = 0.315$, and its basin is shown in gray. As the parameters $a$ and $\varepsilon$ increase, the chaotic attractor and a smooth unstable torus (denoted by a dashed line) on the basin boundary become closer (see Fig. 2(b)). Eventually, when passing the threshold value $(a, \varepsilon) = (1.298\,618, 0.369\,309)$, a sudden destruction of the chaotic attractor occurs through a collision with the smooth unstable torus which is developed from the unstable fixed point of the (unforced) logistic map. This BC corresponds to a natural generalization of the BC occurring for the unforced case ($\varepsilon = 0$). Hence, we call it the "standard" BC.

As $a$ and $\varepsilon$ are increased, the standard BC line continues smoothly. However, at a lower vertex $(a_l^*, \varepsilon_l^*) \simeq (1.227, 0.404)$ (denoted by a plus $(+)$ in Fig. 1(b)), the standard BC line ends and a new kind of BC curve begins by making a sharp turning. Hence, the BC curve loses its differentiability at the vertex. For this case, the standard BC line is continued smoothly beyond the vertex as a curve of a basin metamorphosis line denoted by a dotted line, and the new BC curve joins smoothly with an interior crisis curve denoted by a dashed line at the vertex (see Fig. 1(b)). When passing the basin boundary metamorphosis line, the basin boundary suddenly jumps in size [24], and as the interior crisis curve is crossed, abrupt widening of an attractor occurs [20]. Note that these double (boundary and interior) crises plus a basin boundary metamorphosis occur simultaneously at the vertex [26].

Below the basin boundary metamorphosis line in the tongue, a smooth torus (denoted by a heavy black curve) exists inside an absorbing area bounded by the critical curves $L_k$ ($k = 1, \dots, 4$) (e.g., see Fig. 2(c)

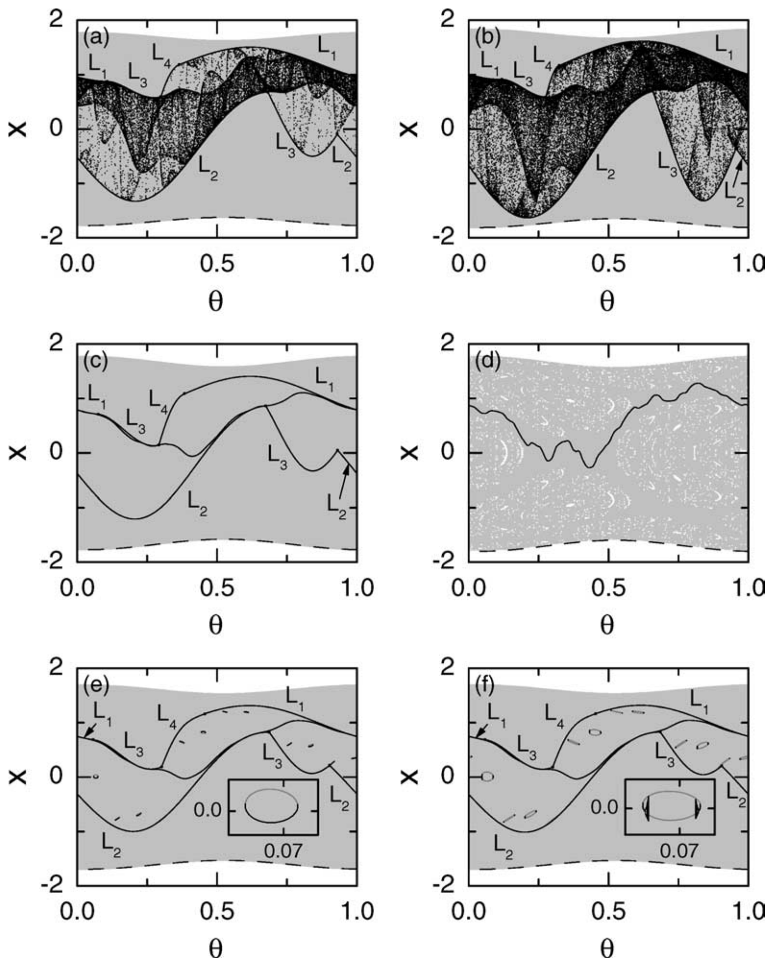


Fig. 2. (a) and (b) Standard BC of a chaotic attractor. Chaotic attractors bounded by the critical curves $L_k$ $(k = 1, \ldots, 4)$ and their basins of attraction are denoted by black dots and shown in gray, respectively for (a) $a = 1.19$ and $\varepsilon = 0.315$ and (b) $a = 1.265$ and $\varepsilon = 0.3525$. Here the dashed line represents a smooth unstable torus on the basin boundary. (c) and (d) Basin boundary metamorphosis. (c) A smooth torus (denoted by a heavy black curve) exists inside the absorbing area bounded by the critical curves $L_k$ $(k = 1, \ldots, 4)$ for $a = 1.05$ and $\varepsilon = 0.355$. (d) "Holes" (denoted by white dots), leading to divergence, appear inside the basin (shown in gray) of the smooth torus (denoted by a heavy black curve) for $a = 1.187$ and $\varepsilon = 0.4235$ after breakup of the absorbing area. (e) and (f) Appearance of a ring-shaped unstable set in the RA of level 7. A smooth torus (denoted by a heavy black curve) and a ring-shaped unstable set exist inside the absorbing area bounded by the critical curves $L_k$ $(k = 1, \ldots, 4)$ for (e) $a = 0.989$ and $\varepsilon = 0.3245$ and (f) $a = 0.993$ and $\varepsilon = 0.3265$. A ring-shaped unstable set is composed of $F_7$ $(= 13)$ small rings. Magnified views of a ring are given in the insets. Note that each ring consists of the unstable part (composed of unstable orbits with the forcing period $F_7$ and shown in dark gray) and the attracting part (denoted by black dots). For more details, see the text.

for $a = 1.05$ and $\varepsilon = 0.355$). However, as the basin boundary metamorphosis line is crossed, the absorbing area becomes broken up through collision with the smooth unstable torus (denoted by the dashed line), and then "holes (denoted by white dots)", leading to divergence, appear inside the basin of the smooth attracting torus (see Fig. 2(d)) [27]. As a consequence of this basin boundary metamorphosis, the smooth unstable torus becomes inaccessible from the interior of basin of the smooth attracting torus, and hence it cannot induce any BC. For this case, using the RAs to the quasiperiodic forcing, we locate an invariant ring-shaped unstable set that causes a new type of BC through a collision with the smooth (attracting) torus. When passing the dash-dotted line in Fig. 1(a), such a ring-shaped unstable set is born via a phase-dependent saddle-node bifurcation [22]. This bifurcation has no counterpart in the unforced case. As an example, we consider the RA of level $k = 7$ and explain the structure of the ring-shaped unstable set. As shown in Fig. 2(e) for $a = 0.989$ and $\varepsilon = 0.3245$, the RA to the smooth torus (denoted by a heavy black line), composed of stable orbits with period $F_7$ $(= 13)$, exists inside an absorbing area bounded by segments of the critical curves $L_k$ $(k = 1, \ldots, 4)$. We also note that a ring-shaped unstable set, consisting of $F_7$ small rings, lies inside the absorbing area. At first, each ring consists of the stable (shown in black) and unstable (shown in dark gray) orbits with the forcing period $F_7$ (see the inset in Fig. 2(e)). However, as the parameters $a$ and $\varepsilon$ increase, such rings evolve, and thus each ring becomes composed of a large unstable part (shown in dark gray) and a small attracting part (denoted by black dots) (see the inset in Fig. 2(f)). As the level $k$ of the RA increases, the ring-shaped unstable set consists of a larger number of rings with a smaller attracting part. Hence, we believe that, in the quasiperiodic limit, the ring-shaped unstable set might become a complicated invariant unstable set composed of only unstable orbits. Through a collision with this ring-shaped unstable set which has no counterpart in the unforced case, a new type of BC occurs, as will be seen below.

With further increase in $a$ and $\varepsilon$, both the new BC curve and the basin boundary metamorphosis line end simultaneously at the upper double-crisis vertex (denoted by a plus) $(a_u^*, \varepsilon_u^*) \simeq (1.154, 0.437)$ in Fig. 1(b). Then, the standard BC line, which joins smoothly with the basin boundary metamorphosis line at the upper vertex, starts again by making an angle. Along the routes $A$ and $B$ beyond the upper vertex, standard BCs of the chaotic attractor and SNA occur, respectively. On the other hand, the new BC curve turns smoothly into a curve of intermittency at the upper vertex. When passing the intermittency line, a transition from a smooth torus to an intermittent SNA occurs through collision with a ring-shaped unstable set [22]. As in the case of interior crisis, the size of the attractor abruptly increases. Hereafter, we will study new type of BCs which occur along the routes $C$, $D$, and $E$ crossing the segment bounded by the lower and upper double-crisis vertices (see Fig. 1(b)). A nonchaotic attractor (smooth torus (route $C$) or SNA (route $D$)) as well as a chaotic attractor (route $E$) is found to be abruptly destroyed through a new BC when it collides with a ring-shaped unstable set.

We now fix the value of $a$ at $a = 1.18$ and investigate the BC of a smooth torus by varying $\varepsilon$ along the route $C$. Fig. 3(a) shows a smooth torus (denoted by black curve) whose basin is shown in gray for $\varepsilon = 0.43$. Due to the existence of holes (shown in white), leading to divergence, the smooth unstable torus (denoted by the dashed line) is not accessible from the interior of the basin of the smooth attracting torus. As the parameter $\varepsilon$ increases, the smooth torus and holes become closer, as shown in Fig. 3(b) for $\varepsilon = 0.445$. Eventually, the smooth (attracting) torus is abruptly destructed via a BC when it collides with the hole boundary for $\varepsilon = \varepsilon^* (= 0.445\,567\,905)$. Using the RA of level $k = 7$, we investigate the mechanism for the BC of the smooth torus. Fig. 3(c) shows the smooth torus (denoted by a black line), the ring-shaped unstable set (represented by dark gray curves), and holes (shown in white) for $\varepsilon = 0.427$. The RAs to the smooth torus and the ring-shaped unstable set are composed of stable and unstable orbits with period $F_7$ $(= 13)$, respectively. For this case, the ring-shaped unstable set is close to the smooth torus. However, it does not lie on any hole boundary (e.g., see a magnified view in Fig. 3(d)). As the parameter $\varepsilon$ increases, the size of holes increases and new holes appear. Then, some part of the ring-shaped unstable set lies on a hole boundary, as shown in Fig. 3(e) and (f). With further increases in $\varepsilon$, the smooth torus and the ring-shaped unstable set on the hole boundary become closer, and eventually, for $\varepsilon = \varepsilon_7^*$ $(= 0.430\,854\,479)$ a phase-dependent saddle-node bifurcation occurs through a collision between the smooth torus and the ring-shaped unstable set. Then, "gaps," where the former attractor (i.e., the stable $F_7$-periodic orbits) no longer exists and almost all trajectories go to the infinity, are formed, as shown in Fig. 3(g) (e.g., see a magnified gap in Fig. 3(h)). As a result, a "partially-destroyed" torus with $F_7$ $(= 13)$ gaps, where divergence occurs, is left. By increasing the level of the RA to $k = 19$, we study the BC of the smooth torus. It is thus found that the threshold value $\varepsilon_k^*$, at which the phase-dependent saddle-node bifurcation of level $k$ (inducing the phase-dependent BCs in the gaps) occurs, converges to the quasiperiodic limit $\varepsilon^*$ $(= 0.445\,567\,905)$ in an algebraic manner,

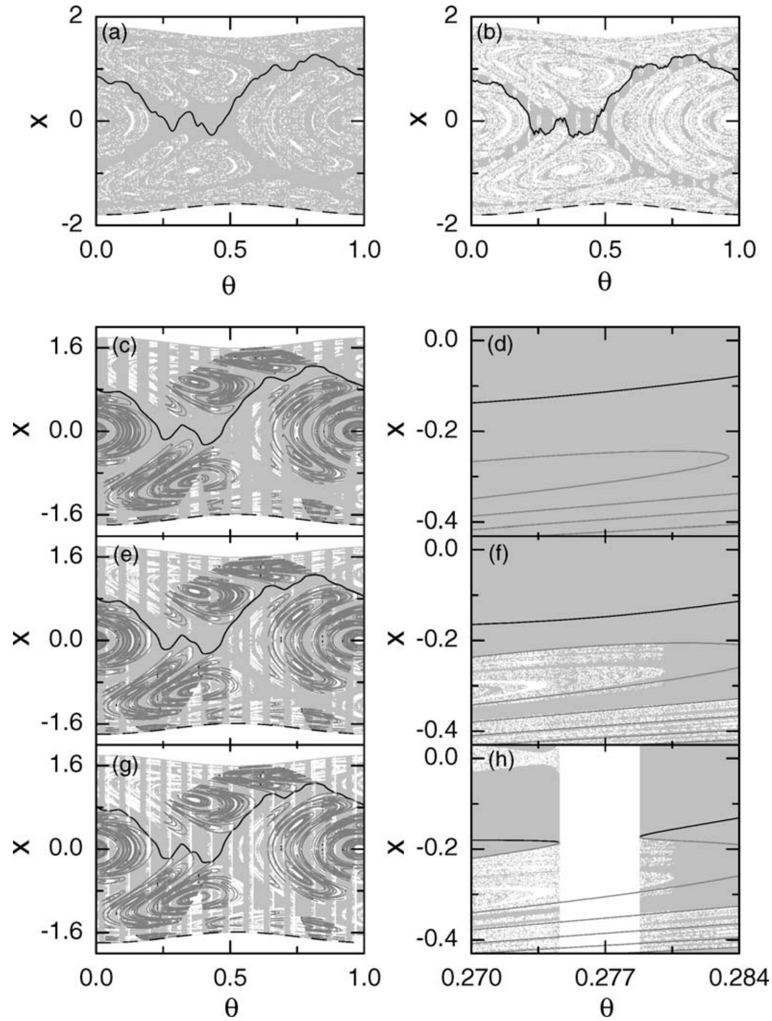


Fig. 3. (a) and (b) BC of a smooth torus along the route $C$ for $a = 1.18$. (a) Smooth torus (denoted by a black curve) and its basin (shown in gray) for $\varepsilon = 0.43$. The unstable smooth torus (denoted by a dashed line) is not accessible from the interior of the basin of the stable smooth torus because of the existence of holes (denoted by white dots). (b) Smooth torus and holes just before the BC for $\varepsilon = 0.445$. (c)–(h) Analysis of the mechanism for the BC of the smooth torus in the RA of level 7 for $a = 1.18$. Magnified views near $(\theta, x) = (0.277, -0.2)$ in (c), (e), and (g) are given in (d), (f), and (h), respectively. Here, the smooth torus whose basin is shown in gray, a ring-shaped unstable set, and holes are shown in black, dark gray, and white dots, respectively. In (c) and (d) for $\varepsilon = 0.427$, a ring-shaped unstable set lies close to the smooth torus. In (e) and (f) for $\varepsilon = 0.43$, some part of the ring-shaped unstable set lies on a hole boundary (e.g., see a magnified view in (f)). For $\varepsilon = \varepsilon_7^*$ $(= 0.430854479)$, a BC occurs via phase-dependent saddle-node bifurcations between the smooth torus and the ring-shaped unstable set on the hole boundary. Then, $F_7$ $(= 13)$ "gaps", where divergence occurs, are formed, as shown in (g) for $\varepsilon = 0.4309$, (e.g., see a magnified gap in (h)).

$|\Delta\varepsilon_k| \sim F_k^{-\alpha}$, where $\Delta\varepsilon_k = \varepsilon_k^* - \varepsilon^*$ and $\alpha \simeq 2.01$. As the level $k$ of the RA increases, the number of gaps, where divergence takes place, becomes larger, and eventually in the quasiperiodic limit, a BC occurs in a dense set of gaps covering the whole $\theta$-range. Consequently, the whole smooth torus disappears suddenly via a new type of BC when it collides with the ring-shaped unstable set.

When crossing the remaining part of the new BC curve along the routes $D$ and $E$ in Fig. 1(b), a SNA and a chaotic attractor are destructed abruptly through a collision with a ring-shaped unstable set, respec-

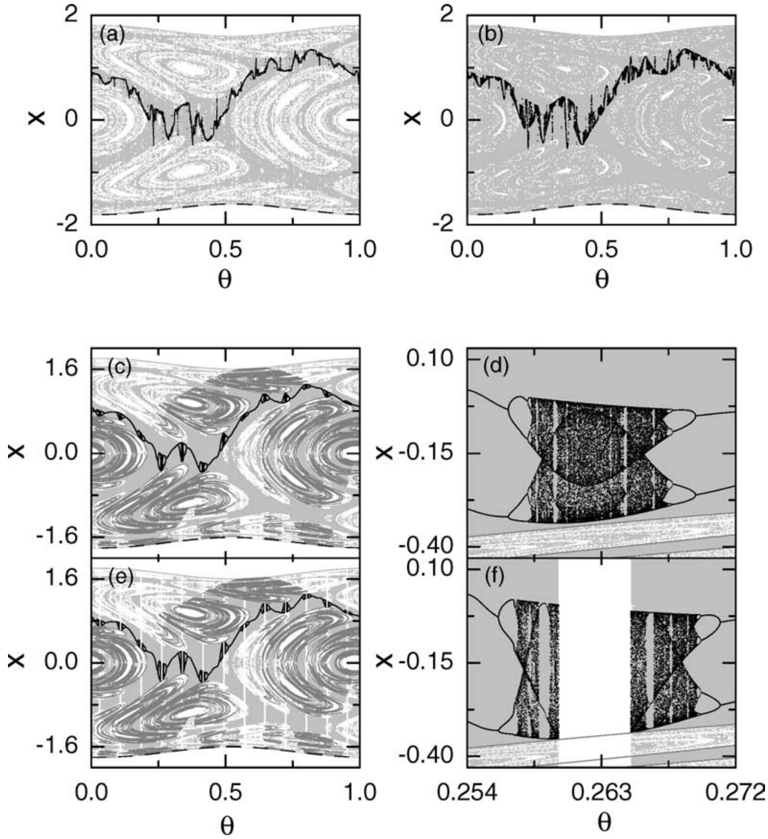


Fig. 4. (a) a SNA with $\sigma_x = -0.038$ and $\delta = 1.077$ and (b) a chaotic attractor $\sigma_x = 0.006$ are denoted by black dots for $(a, \varepsilon) = (1.2327, 0.43)$ and $(1.227, 0.405)$, respectively. These attractors whose basins are shown in gray lie close to holes (represented by white dots), leading to divergence. (c)–(f) Investigation of the mechanism for the BC of the SNA along the route $D$ in the RA of level $k = 7$ for $\varepsilon = 0.43$. The RAs to the SNA and the ring-shaped unstable set are denoted by black and dark gray dots, respectively, in (c) for $a = 1.207$ and $\varepsilon = 0.43$. Some part of the ring-shaped unstable set lies on a hole boundary (shown in white) (e.g., see a magnified view in (d)). For $a = a_7^*$ $(= 1.208\,945\,689)$, a BC occurs through a collision between the chaotic component of the RA to the SNA and the ring-shaped unstable set on the hole boundary. Then, $F_7$ $(= 13)$ "gaps", where divergence takes place, are formed as shown in (e) for $a = 1.21$ (e.g., see a magnified gap in (f)).

tively. For a fixed value of $\varepsilon = 0.43$, a smooth torus is transformed into a SNA via gradual fractalization [14] when passing a threshold value of $a = 1.231\,592$. Fig. 4(a) shows a SNA (denoted by black dots) with $\sigma_x = -0.038$ and $\delta = 1.077$ for $a = 1.2327$. Due to the existence of holes (shown in white), the smooth unstable torus (represented by a dashed line) is inaccessible from the interior of the basin of the SNA. As $a$ passes another threshold value $a^*$ $(= 1.232\,722\,002)$, the SNA is destroyed abruptly via a BC when it collides with a hole boundary. As in the case of the SNA, BC of a chaotic attractor also occurs along the route $E$ through a collision with a hole boundary. For example, at a fixed value of $\varepsilon = 0.405$, consider a chaotic attractor with $\sigma_x = 0.006$ shown in Fig. 4(b) for $a = 1.227$. Sudden destruction of the chaotic attractor takes place when passing a threshold value of $a = 1.227\,030\,014$. For this case, the mechanism for the BC of the chaotic attractor is the same as that for the case of the SNA. Hence, it is sufficient to consider only the case of the SNA for presentation of the mechanism for the BC. Using the RA of level $k = 7$, we investigate the mechanism for the BC of the SNA along the route $D$ for $\varepsilon = 0.43$. Fig. 4(c) and (d) show the RAs to the SNA (denoted by black dots) and the ring-shaped unstable set (shown in dark gray). Unlike the case of the smooth torus, the RA to the SNA consists of the periodic and chaotic components. Since the periodic component is dominant, the average Lyapunov exponent ($\langle \sigma_x \rangle = -0.109$) is negative, where $\langle \cdots \rangle$ denotes the average over the whole $\theta$. Note that some of the ring-shaped unstable set lies on a hole boundary (shown in white) (e.g., see a magnified view in Fig. 4(d)). As $a$ is increased, the chaotic component of the RA to the SNA and the ring-shaped unstable set on the hole boundary become closer. Eventually, for $a = a_7^*$ ($= 1.208\,945\,689$), they make a collision and then a phase-dependent BC occurs. Thus, $F_7$ ($= 13$) gaps, where divergence occurs, are formed in the whole range of $\theta$, as shown in Fig. 4(e) for $a = 1.21$ (e.g., see a magnified gap in Fig. 4(f)). As a result, the SNA becomes destroyed partially in gaps. By increasing the level of the RA to $k = 19$, we study the BC of the SNA. It is thus found that the threshold value $a_k^*$, at which the phase-dependent BC of level $k$ occurs, converges to the quasiperiodic limit $a^*$ ($= 1.232\,722\,002$) in an algebraic manner, $|\Delta a_k| \sim F_k^{-\alpha}$, where $\Delta a_k = a_k^* - a^*$ and $\alpha \simeq 2.67$. As the level $k$ of the RA increases, more and more gaps, where divergence takes place, appear, and eventually in the quasiperiodic limit, a BC occurs in a dense set of gaps covering the whole $\theta$-range. Hence, the whole SNA is destroyed abruptly through a new type of BC when it collides with the ring-shaped unstable set.

## 3. Summary

Using the RAs to the quasiperiodic forcing, we have investigated the mechanism for the BCs in the quasiperiodically forced logistic map which is a representative model for the quasiperiodically forced period-doubling systems. As the quasiperiodic forcing amplitude $\varepsilon$ passes a threshold value, a basin boundary metamorphosis occurs, and then the smooth unstable torus, inducing the standard BC, becomes inaccessible from the interior of the basin of the attractor. For this case, a new type of BC has been found to occur through a collision with a ring-shaped unstable set which has no counterpart in the unforced case. As a result, a nonchaotic attractor (smooth torus or SNAs) as well as a chaotic attractor is abruptly destroyed. Finally, we note that this kind of new BC occurs in typical quasiperiodically forced period-doubling systems such as the quasiperiodically forced Hénon map [20].

## Acknowledgements

S.Y.K. thanks A. Jalnine for fruitful discussions on dynamical transitions in quasiperiodically forced systems. This work was supported by the 2004 Research Program of the Kangwon National University.

## References

[1] C. Grebogi, E. Ott, J.A. Yorke, Phys. Rev. Lett. 48 (1982) 1507; C. Grebogi, E. Ott, J.A. Yorke, Physica D 7 (1983) 181.
[2] C. Grebogi, E. Ott, F. Romeiras, J.A. Yorke, Phys. Rev. A 36 (1987) 5365; C. Grebogi, E. Ott, J.A. Yorke, Phys. Rev. Lett. 57 (1986) 1284.
[3] C. Jeffries, J. Perez, Phys. Rev. A 27 (1983) 601; S.D. Brorson, D. Dewey, P.S. Linsay, Phys. Rev. A 28 (1983) 1201; H. Ikezi, J.S. Degrassie, T.H. Jensen, Phys. Rev. A 28 (1983) 1207; R.W. Rollins, E.R. Hunt, Phys. Rev. A 29 (1984) 3327; E.G. Gwinn, R.M Westervelt, Phys. Rev. Lett. 54 (1985) 1613; M. Iansiti, Q. Hu, R.M. Westervely, M. Tinkham, Phys. Rev. Lett. 55 (1985) 746; D. Dangoisse, P. Glorieux, D. Hennequin, Phys. Rev. Lett. 57 (1986) 2657; W.L. Ditto, S. Rauseo, R. Cawley, C. Grebogi, G.-H. Hsu, E. Kostelich, E. Ott, H.T. Savage, R. Segnan, M.L. Spano, J.A. Yorke, Phys. Rev. Lett. 63 (1989) 923; J.C. Sommerer, W.L. Ditto, C. Grebogi, E. Ott, M.L. Spano, Phys. Lett. A 153 (1991) 105.
[4] A. Prasad, S.S. Negi, R. Ramaswamy, Int. J. Bifur. Chaos 11 (2001) 291.
[5] C. Grebogi, E. Ott, S. Pelikan, J.A. Yorke, Physica D 13 (1984) 261.
[6] F.J. Romeiras, E. Ott, Phys. Rev. A 35 (1987) 4404; M. Ding, C. Grebogi, E. Ott, Phys. Rev. A 39 (1989) 2593.
[7] T. Kapitaniak, E. Ponce, T. Wojewoda, J. Phys. A 23 (1990) L383.
[8] J.F. Heagy, S.M. Hammel, Physica D 70 (1994) 140.
[9] A.S. Pikovsky, U. Feudel, Chaos 5 (1995) 253, see Eqs. (11)–(14) for the definition of the phase sensitivity exponent $\delta$.
[10] O. Sosnovtseva, U. Feudel, J. Kurths, A. Pikovsky, Phys. Lett. A 218 (1996) 255.
[11] U. Feudel, J. Kurths, A.S. Pikovsky, Physica D 88 (1995) 176; U. Feudel, C. Grebogi, E. Ott, Phys. Rep. 290 (1997) 11.
[12] S.P. Kuznetsov, A.S. Pikovsky, U. Feudel, Phys. Rev. E 51 (1995) R1629; S. Kuznetsov, U. Feudel, A. Pikovsky, Phys. Rev. E 57 (1998) 1585; S. Kuznetsov, E. Neumann, A. Pikovsky, I. Sataev, Phys. Rev. E 62 (2000) 1995; S.P. Kuznetsov, Phys. Rev. E 65 (2002) 066209.
[13] P.R. Chastell, P.A. Glendinning, J. Stark, Phys. Lett. A 200 (1995) 17;

H. Osinga, J. Wiersig, P. Glendinning, U. Feudel, Int. J. Bifur. Chaos 11 (2001) 3085.

[14] T. Nishikawa, K. Kaneko, Phys. Rev. E 54 (1996) 6114.

[15] T. Yalçınkaya, Y.-C. Lai, Phys. Rev. Lett. 77 (1996) 5039.

[16] A. Prasad, V. Mehra, R. Ramaswamy, Phys. Rev. Lett. 79 (1997) 4127;
A. Prasad, V. Mehra, R. Ramaswamy, Phys. Rev. E 57 (1998) 1576.

[17] A. Witt, U. Feudel, A. Pikovsky, Physica D 109 (1997) 180.

[18] A. Venkatesan, M. Lakshmanan, A. Prasad, R. Ramaswamy, Phys. Rev. E 61 (2000) 3641;
A. Venkatesan, M. Lakshmanan, Phys. Rev. E 63 (2001) 026219.

[19] S.S. Negi, A. Prasad, R. Ramaswamy, Physica D 145 (2000) 1.

[20] H.M. Osinga, U. Feudel, Physica D 141 (2000) 54.

[21] B.R. Hunt, E. Ott, Phys. Rev. Lett. 87 (2001) 254101;
J.-W. Kim, S.-Y. Kim, B. Hunt, E. Ott, Phys. Rev. E 67 (2003) 036211.

[22] S.-Y. Kim, W. Lim, E. Ott, Phys. Rev. E 67 (2003) 056203;
S.-Y. Kim, W. Lim, J. Phys. A 37 (2004) 6477.

[23] W.L. Ditto, M.L. Spano, H.T. Savage, S.N. Rauseo, J. Heagy, E. Ott, Phys. Rev. Lett. 65 (1990) 533;
T. Zhou, F. Moss, A. Bulsara, Phys. Rev. A 45 (1992) 5394;
W.X. Ding, H. Deutsch, A. Dinklage, C. Wilke, Phys. Rev. E 55 (1997) 3769;
T. Yang, K. Bilimgut, Phys. Lett. A 236 (1997) 494;
B.P. Bezruchko, S.P. Kuznetsov, Y.P. Seleznev, Phys. Rev. E 62 (2000) 7828.

[24] C. Grebogi, E. Ott, J.A. Yorke, Phys. Rev. Lett. 56 (1986) 1011;
C. Grebogi, E. Ott, J.A. Yorke, Physica D 24 (1987) 243.

[25] C. Mira, L. Gardini, A. Barugola, J.-C. Cathala, Chaotic Dynamics in Two-Dimensional Noninvertible Maps, World Scientific, Singapore, 1996.

[26] J.A. Gallas, C. Grebogi, J.A. Yorke, Phys. Rev. Lett. 71 (1993) 1359;
H.B. Stewart, Y. Ueda, C. Grebogi, J.A. Yorke, Phys. Rev. Lett. 75 (1995) 2478.

[27] U. Feudel, A. Witt, Y.-C. Lai, C. Grebogi, Phys. Rev. E 58 (1998) 3060.